

EventBind: Learning a Unified Representation to Bind Them All for Event-based Open-world Understanding

Jiazhou Zhou¹, Xu Zheng¹, Yuanhuiyi Lyu¹, and Lin Wang^{1,2}*

¹ Hong Kong University of Science and Technology, Guangzhou, China
 {jiazhouzhou,yuanhuiyilyu}@hkust-gz.edu.cn, zhengxu128@gmail.com

² Hong Kong University of Science and Technology, Hong Kong, China
 linwang@ust.hk

Project Page: <https://vlislab22.github.io/EventBind/>

Abstract. In this paper, we propose EventBind, a novel and effective framework that unleashes the potential of vision-language models (VLMs) for event-based recognition to compensate for the lack of large-scale event-based datasets. In particular, due to the distinct modality gap with the image-text data and the lack of large-scale datasets, learning a common representation space for images, texts, and events is non-trivial. Intuitively, we need to address two key challenges: 1) how to generalize CLIP’s visual encoder to event data while fully leveraging events’ unique properties, *e.g.*, sparsity and high temporal resolution; 2) how to effectively align the multi-modal embeddings, *i.e.*, image, text, and events. Accordingly, we first introduce a novel event encoder that subtly models the temporal information from events and meanwhile generates event prompts for modality bridging. We then design a text encoder that generates content prompts and utilizes hybrid text prompts to enhance EventBind’s generalization ability across diverse datasets. With the proposed event encoder, text encoder, and image encoder, a novel Hierarchical Triple Contrastive Alignment HTCA module is introduced to jointly optimize the correlation and enable efficient knowledge transfer among the three modalities. We evaluate various settings, including fine-tuning and few-shot on three benchmarks and our EventBind achieves new state-of-art accuracy compared with the previous methods, such as on N-Caltech101 (+5.34% and +1.70%) and N-Imagenet (+5.65% and +1.99%) with fine-tuning and 20-shot settings respectively. Moreover, our EventBind can be flexibly extended to the event retrieval task using text or image queries, showing plausible performance.

Keywords: Event Camera · Multi-modal · Object Recognition

1 Introduction

Event cameras are bio-inspired sensors [20, 74] that have recently received much attention in the computer vision and robotics community for their distinct mer-

* Corresponding author

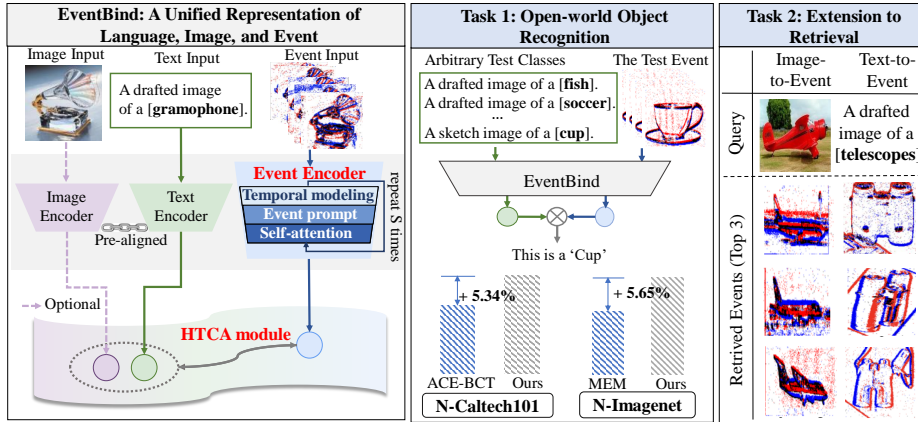


Fig. 1: Overview of our EventBind, which extracts the events’ high temporal and sparse spatial information via the proposed Event Encoder and aligns event, image, and text embeddings in the unified representation space with a novel Hierarchical Triple Contrastive Alignment (HTCA) module. EventBind solves various practical tasks like open-world object recognition and few-shot object recognition with significant performance improvements compared to the previous best models [32, 40]. Our EventBind framework can be flexibly extended to image-to-event and text-to-event retrieval tasks.

its, such as high temporal resolution and no motion blur. Event cameras perceive the per-pixel brightness changes asynchronously and output event streams, encoding the time, pixel location, and polarity of intensity changes. This distinct feature has sparked many research endeavors targeted at event cameras, and recently deep neural networks (DNNs) have been applied to event-based vision, showing significant performance gains for many tasks, such as object recognition [21, 24, 29, 34, 38, 40, 60]. Event cameras pose superior performance in capturing objects in dynamic environments; however, learning high-performance DNNs for event data is often impeded by the asynchronous nature of events and the challenge of obtaining high-quality and large-scale labeled datasets [20, 64, 74]. Moreover, in real-world scenarios, DNN model failures may occur when encountering event data with new categories not present in the training set. Nonetheless, retraining large models for each new category is impractical, making it necessary to explore zero-shot and few-shot recognition pipelines for event cameras.

Recently, vision-language models (VLMs), *e.g.*, CLIP [50], have shown promising open-world performance on the 2D image-based recognition tasks. Benefiting from large-scale training data (over 400M image-text pairs), CLIP can serve as the pre-trained model and be transferred to other visual data, *e.g.*, video [45, 51, 63] and depth [73], under the few-shot setting. Intuitively, we ask a question: how to transfer the pre-trained CLIP to the event data and achieve open-world few-shot recognition performance while considering its asynchronous feature and the distinct modality shift from the image and text data? To this end, we strive to address two crucial challenges. **1)** how to generalize CLIP’s

visual encoder to the event data while fully leveraging events’ unique properties, *e.g.*, sparsity and high temporal resolution. That is, the distinct modality discrepancy of event data, compared with the canonical images, makes it difficult to directly extract the spatial-temporal features if using CLIP’s visual encoders. **2)** how to effectively align the multi-modal embeddings, *i.e.*, image, text, and event. The significant modality gap between them poses obstacles to reliable and effective feature alignments.

In this paper, we propose EventBind, a novel framework that unleashes the potential of CLIP for event-based recognition tasks to compensate for the lack of large-scale event-based datasets. Our EventBind consists of an event encoder, a text encoder, and the CLIP image encoder, as illustrated in Fig. 1. Our method enjoys three key technical breakthroughs. Firstly, we introduce an event encoder to address the challenge of generalizing CLIP’s original visual encoder to the event data (Sec. 3.1). The event encoder incorporates event temporal modeling and event prompts generation to better exploit events’ unique properties, such as sparsity and high temporal resolution. Specifically, the event temporal modeling enables temporal information exchange between event frames, while the generated event prompts are used to capture the spatial-temporal information of raw events. To better align text with events, we introduce a new text encoder in our EventBind, building upon the basic text encoder in CLIP (Sec. 3.2). The text encoder generates content prompts to improve the fine-tuning performance with a lightweight MLP network and incorporates hybrid text prompts —combining hand-crafted and learnable prompts —to enhance the generalization across diverse datasets. Moreover, we introduce an additional loss function to ensure consistency between the hand-crafted and learnable prompts.

To tackle the second challenge, we propose a Hierarchical Triple Contrastive Alignment (HTCA) module to align the multi-modal feature embeddings, *i.e.*, events, image, and text to learn a unified feature representation (Sec. 3.3). Concretely, multi-modal triple feature alignment is conducted to jointly align the text, events, and image by minimizing the contrastive loss between each two of them. Meanwhile, it imposes the semantic feature alignment to keep the semantic consistency between the events and image. In a nutshell, with the HTCA module, we can effectively bridge the modality gap and facilitate efficient knowledge transfer among the three modalities.

We conduct extensive experiments to evaluate our EventBind on three event-based recognition benchmarks: N-Caltech101, N-MNIST, and N-ImageNet, covering fine-tuning and few-shot settings. The experimental results demonstrate that our EventBind significantly outperforms the existing methods by a large margin (Tab. 1 and Tab. 2) and the proposed event encoder shows superior efficiency (Tab. 6), thus enhancing downstream tasks in event-based vision. Additionally, we demonstrate that our EventBind can be flexibly extended to the application of the event retrieval tasks by utilizing both text and image queries, which further spotlights EventBind’s transferability and versatility.

In summary, our main contributions are as follows: **(I)** We propose EventBind, a novel framework that unleashes the potential of CLIP for event-based

recognition to compensate for the lack of large-scale datasets. **(II)** We propose a novel event encoder and a text encoder to harness properties of events (*e.g.*, high temporal resolution) and to enhance the EventBind’s generalization ability, respectively. **(III)** We propose a novel Hierarchical Triple Contrastive Alignment (HTCA) module that jointly optimizes the correlation alignment among three modalities. **(IV)** We demonstrate that our EventBind outperforms existing methods by a significant margin in both fine-tuning and few-shot settings on three event recognition benchmarks. As a penitential, our EventBind can also be freely extended to the event retrieval task when employing text or image queries.

2 Related Works

Vision-language Models (VLMs). VLMs gain interest for their cross-modal transfer ability, focusing on aligning image-text embeddings rather than just image data. As a pioneering work, CLIP [50] employs contrastive learning objectives on image-text pairs and achieves impressive zero-shot classification on 30+ datasets. Motivated by this, other works have aligned the original image and text with different types of modalities, such as audio [43], 3D point clouds [10, 65, 71, 72], video [45, 51, 63], and depth [73]. In short, methods can be split into three types: 1) Single-encoder framework with frozen CLIP visual encoder as backbone [27, 39]; 2) Dual-encoder framework using CLIP’s text and fine-tuned visual encoder for added modality [41, 45, 51, 63, 72, 73]; 3) Triple-encoder framework with CLIP’s text and visual encoders and new encoder for additional modality embeddings [43, 65, 71]. However, there are few attempts to align event modality with image and text. One concurrent work called EventCLIP [64] exploits the gray-scale event frame as the intermediate representation of event data and utilizes the CLIP visual encoder for event embeddings. Our EventBind differs from [64] in three main aspects: 1) EventBind proposes a tailored event encoder instead of CLIP’s image encoder; 2) EventBind creates a unified representation space for event, image, and text, unlike EventCLIP which only aligns event with text; 3) EventBind shows effectiveness in event retrieval alongside object recognition.

Prompt Learning for VLMs. Prompt learning plays a pivotal role in harnessing the power of large-scale VLMs [10, 18]. Existing research focuses on creating prompts for VLMs that consider both vision and language. Text prompts activate specific capabilities of VLMs through designed templates or learnable embeddings. [50, 67, 75, 76]. These prompts guide VLMs in cross-modal understanding, yielding promising results on various tasks [35, 36, 54, 56, 61]. Visual prompts tuning injects a small number of learnable parameters into input space [28], enhancing the performance of VLMs [3, 6, 70] and enabling rapid adaptation to downstream tasks [4, 26]. Compared to text prompts, visual prompts can be flexibly presented in various forms, such as bounding boxes [3, 37], colored blocks [68], positions [58] and points [31]. In EventBind, we create event prompts to help the model learn event data features.

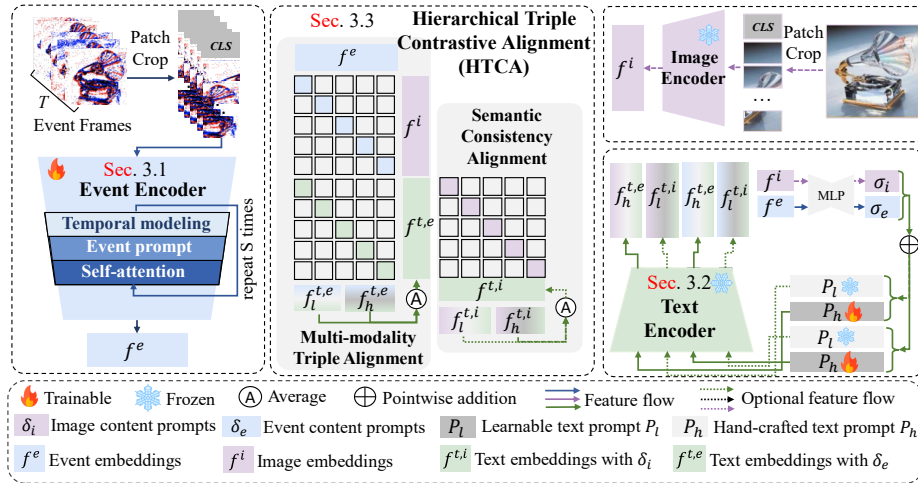


Fig. 2: Overview framework of EventBind, which consists of image encoder pre-aligned with text encoder and the proposed event encoder. It takes image(optional), text, and event as input, generating the image embeddings f^i , event embeddings f^e and text embeddings $f^{t,e}, f^{t,i}$. Then all output embeddings are aligned in the HTCA module to establish a unified representation space.

Event-based Recognition. Event cameras excel in high-temporal resolution, low latency, and very high dynamic range, making them ideal for real-time object recognition in applications like autonomous vehicles and mobile systems [74]. However, event data’s unique traits hinder the direct use of pre-trained models. For this reason, various methods [1, 5, 8, 15, 20, 22, 24, 29, 38, 40, 55, 60, 74] have been proposed. However, learning high-performance DNNs for event data is challenging due to the asynchronous nature of events and the lack of large-scale labeled datasets [74]. Besides, DNNs may fail with new event categories, and retraining large models for each new category is impractical, so few-shot recognition pipelines for event cameras need to be explored. Intuitively, we propose EventBind with novel event encoders and specialized text prompts, buttressed by the HTCT module for effective event-based recognition.

3 Proposed Approach

The proposed EventBind framework is presented in Fig. 2, aiming at unleashing the potential of CLIP for event-based recognition tasks to compensate for the scarcity of large-scale event-based datasets. To this end, our EventBind addresses two technical challenges: 1) how to generalize the CLIP’s visual encoder to the event data while fully exploiting the event’s unique properties, *e.g.*, spatial sparsity and high temporal resolution; 2) how to effectively align the multi-modal embeddings, *i.e.*, image, text, and event, to establish a unified representation space while preserving CLIP’s exceptional few-shot capability.

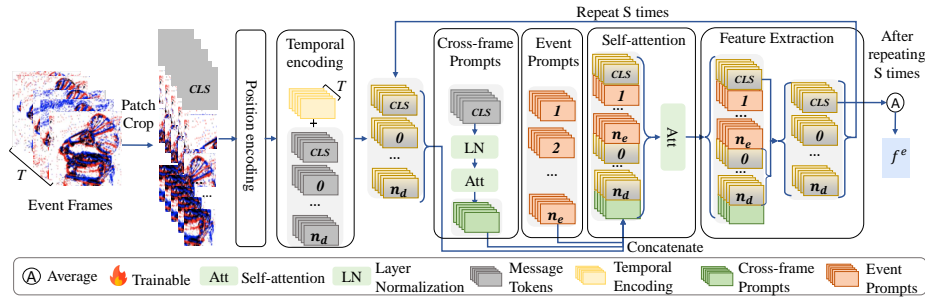


Fig. 3: The architecture of our event encoder consists of two key technical parts: (a) Temporal modeling consisting of temporal encoding and cross-frame prompts for event spatial-temporal modeling by introducing information exchange between event frames; (b) Event prompts generate event modality prompts to provide additional parameters for modality bridging.

Consequently, we design our EventBind consisting of four major components, as depicted in Fig. 2: 1) the event encoder, responsible for extracting dense temporal and sparse spatial information from events and bridging the modality gap (Sec. 3.1); 2) the text encoder (Sec. 3.2) incorporates the event and image content and pre-trained generalizing knowledge from CLIP to generate the text embeddings for enhance performance; 3) the original CLIP’s image encoder for semantically aligned image embeddings³; 4) The hierarchical triple contrastive alignment (HTCA) module (Sec. 3.3) jointly optimizes the correlation among the three distinct modalities, forming a unified embedding space among image, text, and event. In the following sections, we describe these technical components.

3.1 Event Encoder

Event Encoder is designed to transfer the remarkable capability of CLIP to the asynchronous event-based vision. However, addressing the modality disparity among events, images, and text data is nontrivial. In this regard, it is crucial to design a tailored event encoder, which can fully leverage events’ unique properties, such as high temporal information and sparsity. We propose a novel event encoder, that consists of two key technical parts: 1) event temporal modeling to effectively exploit the unique temporal information among event frames and 2) event prompts generation as additional modality-bridging parameters without introducing excessive parameters, thus enabling its efficiency and transferability.

Specifically, we transform the raw event into a series of event frames $I_e \in \mathbb{R}^{T \times H \times W \times 3}$ with T frames of spatial size $H \times W$ (See more details of event frame representation in the suppl.). Then each frame is divided into L non-overlapping $P \times P$ square patches, where $L = H \times W / P^2$. For each event frame, all patches

³ As the image encoder in EventBind remains identical to CLIP, we do not elaborate on it in the following subsection. Note that the image input is optional.

are flattened into a $3P^2$ -dimension vector and presented as $\{x_{t,i} \in \mathbb{R}^{3P^2}\}_i^L$, where t denotes the frame number and i represents the patch number. All patch vectors are projected to D dimension by the matrix multiplication with the linear projection $P_{emb} \in \mathbb{R}^{3P^2 \times D}$. Besides, the additional class token, namely CLS , is concatenated at the beginning of the patch token sequence for each frame. The input token sequence $z_t \in \mathbb{R}^{(L+1) \times D}$ of event frame t can be formulated as:

$$z_t = LN([CLS, P_{emb}^T x_{t,1}, P_{emb}^T x_{t,2}, \dots, P_{emb}^T x_{t,L}]), \quad (1)$$

where $LN(\cdot)$ represents the layer normalization, $[.]$ means the concatenation operation; $x_{t,L}$ denotes the original message tokens, where t is the event frame number and L is the total number of patches.

Event Temporal Modeling. To model the unique temporal correlation among event frames, we add the temporal encoding e with the input token sequence z_t of the event encoder, where $e = e_{spatial} + e_{temporal}$. $e_{spatial}$ and $e_{temporal}$ denote the spatial and temporal positional encoding, respectively. Following CLIP [50], $e_{spatial}$ and $e_{temporal}$ are learnable parameters and randomly initialized. Despite the temporal encoding, the event encoder also introduces cross-frame prompts to exchange information among event frames for better temporal information transmission. Concretely, shown in Fig. 3, for the s -th layer of the event encoder, the class tokens among all T event frames are extracted from the input sequence $z_t^s, t = 1, 2, \dots, T$ and then fed into a norm layer [2] and self-attention [57] successively, aiming at obtaining the s -th layer cross frame prompts $x_{cf}^{s,t}$ as follows:

$$x_{cf}^{s,t} = \text{Att}(\text{LN}([x_{cf}^{s,1}, x_{cf}^{s,2}, \dots, x_{cf}^{s,T}])), \quad (2)$$

where $[.]$ is the concatenation operation. As shown in Fig. 3 green rectangles, the obtained cross-frame prompts, which perceive the temporal relation among frames, are concatenated with the original token sequence z_t^s as the input of the next $(s+1)$ -th layer of the event encoder.

Event Prompts Generation. Based on the event temporal modeling, the unique temporal correlation among event frames is captured. Since fine-tuning the pre-trained image encoder for processing event data may not guarantee good performance because of the modality gap and smaller event dataset size compared to the web-scale image dataset, we propose the event prompts to bridge the modality gaps among the image, text, and event modalities without introducing excessive parameters, which may cause catastrophic forgetting [28]. Specifically, we insert a small number of learnable parameters at the input of each encoder layer. The proposed event prompts P_e are learnable vectors inserted at the output token sequence between the original class token and other message tokens (see orange rectangles in Fig. 3). After event temporal modeling and event prompts generation, we concatenate the original message token $Z^{s,t}$, event prompts $P_e^{s,t}$ and cross-frame prompts $x_{cf}^{s,t}$ then send it into a standard self-attention layer as:

$$z_t^{s+1} = \text{Att}([CLS, P_e^{s,t}, Z^{s,t}, x_{cf}^{s,t}]), \quad (3)$$

where $P_e^{s,t}$ are the event modality prompts for the t -th frame in the s -th layer and $P_e^{s,t} = [p_1^{s,t}, p_2^{s,t}, \dots, p_{n_e}^{s,t}]$; n_e is the number of event modality prompts; $Z^{s,t}$ is the

original message token without the first class token and $Z^{s,t} = [x_1^{s,t}, x_2^{s,t}, \dots, x_{n_d}^{s,t}]$; n_d is the number of the original message token; $x_{cf}^{s,t}$ is the cross-frame event prompts; $\text{Att}(\cdot)$ indicates the self-attention layer. Then, we extract the message tokens as the input of the next $(s + 1)$ -th layer of the event encoder (See Fig. 3 feature extraction block). Let the event encoder E_e with S layers, the above process iterates S times. In the end, we extract the CLS tokens from the token sequence and then project them to the D' dimension using the linear projection $P_{cls} \in \mathbb{R}^{D \times D'}$. The event embeddings f^e are ultimately produced by averaging the CLS token among T event frames.

3.2 Text Encoder

Hybrid Text Prompts After extracting event embeddings based on the event encoder, we subsequently employ hybrid text prompts [67] to enhance model generalization ability across diverse dataset: 1) the hand-crafted text prompt 'A drafted image of a [class].', where [class] represents the category name. Each word is encoded into a D_p -dimension word embeddings, forming the final text token P_h ; 2) the learnable text prompt $P_l = [P_1, P_2, \dots, P_{n_l}, P_{class}]$, where $i = 1, 2, \dots, n_l$ is a random initialized parameter with D_p dimensions; n_l denotes the number of the learnable text prompts; P_{class} represents the word embeddings of [class] and $[\cdot]$ means the concatenation operation.

Content Prompts Besides, the content prompts are introduced to enhance the model performance. The content prompts are generated by a simple two-layer MLP. Specifically, MLP takes the event embeddings f^e and image embeddings f^i as input and produces the corresponding event content prompts $\sigma_e \in \mathbb{R}^{1 \times D_p}$ and the image content prompts $\sigma_i \in \mathbb{R}^{1 \times D_p}$, both of which have the same dimension D_p as the hand-crafted text token P_h . Next, the learnable text prompts P_l and the hand-crafted text prompts P_h are pointwisely added with the content prompts $\sigma_m, m = i, e$, respectively, generating the final text input, as depicted in Fig. 2. Next, the learnable text embeddings $f_l^{t,m}, m = i, e$ and hand-crafted text embeddings $f_h^{t,m}, m = i, e$ with content prompts are generated by the text encoder E_t . Finally, the text embeddings $f^{t,m}, m = e, i$ of modality m is obtained by averaging the $f_l^{t,m}$ and $f_h^{t,m}$.

3.3 Hierarchical Triple Contrastive Alignment (HTCA)

With the extracted event embeddings f^e (Sec. 3.1), image embeddings f^i , and text embeddings with event content prompt $f^{t,e}$ (Sec. 3.2), it's still an open question to bridge the modality gap among the three distinct modalities *i.e.*, image, text, and event, and effectively align them. A simple objective is to align f^e with f^t from scratch. However, the relatively small event dataset and limited vocabulary may hinder reliable representation and plausible few-shot performance. To this end, we propose the Hierarchical Triple Contrastive Alignment (HTCA) module, aiming at aligning the event, image, and text modalities jointly and enhancing model performance based on semantic consistency.

Multi-modality Triple Alignment We first minimize the contrastive loss $L(f^i, f^e)$ between the event embeddings f^e and image embeddings f^i , as well as minimizing $L(f^e, f^{t,e})$ between the event embeddings $f^{t,e}$ and text embeddings with event content prompts $f^{t,e}$. We ignore the image-text pair because we empirically observe that altering the pre-trained image-text alignment reduces performance. Specifically, the contrastive loss is obtained by averaging the whole mini-batch among each pair of modalities M_1 and M_2 , which can be formulated as follows:

$$L(M^1, M^2) = \frac{1}{N} \sum_{n \in N} -\log \frac{\exp(M_n^1 \cdot M_n^2 / \tau)}{\exp(M_n^1 \cdot M_n^2 / \tau) + \sum_{m \in N, m \neq n} \exp(M_n^1 \cdot M_m^2 / \tau)}, \quad (4)$$

where τ is the temperature coefficient, N represents the size of the mini-batch, n, m denote the n -th and the m -th data of the mini-batch, $m \neq n$ and $m = n$ indicates the negative pair and the positive pair in a batch respectively.

Semantic Consistency Alignment. Semantic consistency indicates that embeddings generated from different modalities of the same item share the same semantic meaning, *e.g.* paired text and event data, resulting in the distance between them being closer in representation space. In light of this, we propose the semantic consistency alignment to enhance the model performance and inherit the remarkable few-shot ability of the pre-trained CLIP (Sec. 4.3). Specifically, we ensure the semantic consistency between the image and event content added text embeddings $f^{t,i}$ and $f^{t,e}$ by employing loss function $L(f^{t,i}, f^{t,e})$, as well as additional $MSE(f_l^{t,m}, f_h^{t,m})$ loss to reduce the gap between text embeddings $f_l^{t,m}$ and $f_h^{t,m}$ generated by the learnable and hand-crafted prompts (Sec. 3.2).

3.4 Total Objective

In summary, as shown in Fig. 2, the total objective is composed of $L(f^i, f^e)$, $L(f^e, f^{t,e})$, as well as $L(f^{t,i}, f^{t,e})$ and $MSE(f_l^{t,m}, f_h^{t,m})$, all mentioned in Sec. 3.3. We combine them with different trade-off hyper-parameters:

$$L_{final} = \alpha L(f^i, f^e) + \beta L(f^e, f^{t,e}) + \theta L(f^{t,i}, f^{t,e}) + \gamma MSE(f_l^{t,m}, f_h^{t,m}), \quad (5)$$

where $f^e, f^i, f^{t,e}, f^{t,i}$ denotes the event embeddings, image embeddings, event content added text embeddings and image content added text embeddings; $MSE(\cdot)$ indicates the mean squared error loss function; $f_l^{t,m}$ and $f_h^{t,m}$ is the text embeddings generated from the learnable and hand-crafted text prompts with modality m content prompts, respectively, where m can be e for event modality or i for image modality. We set the default values of α, β, θ , and γ to 1 as the frozen CLIP visual encoder serves as the initialization of the event encoder, ensuring the magnitudes of the four components distributed on the same scale. Note that when the image input is unavailable, only $L(f^e, f^{t,e})$ participates in backpropagation, namely setting α, θ , and γ to 0 and β to 1.

4 Experiments and Evaluation

4.1 Experimental Setup and Datasets

Dataset. We use three public image-event-text paired datasets for our experiments: N-ImageNet [29] with ImageNet-1K [13], N-Caltech101 [19] with Caltech101 [46], and N-MNIST [46] with MNIST [14]. We split N-ImageNet and N-MNIST officially. N-Caltech101 is split 4:1 for training and validation. The same validation set is used for zero-shot, few-shot, and fine-tuning. Few-shot data are randomly selected and consistent. *See more details on experimental settings in the Suppl.*

Dataset Preprocessing. RGB images are resized to 224×224 resolution to ensure consistency with ViT input settings, while grayscale images are transformed into a three-channel tensor by concatenating three identical copies. Then we transform the event data into event frames, with the aggregated event counts per frame N being determined by hyperparameter search. *See more discussion on N in Sec. 4.3 and the details of event frame representation in suppl.*

Inference and Task Settings. Event recognition indicates the classification of event data, which is a fundamental task in event-based vision. As shown in Fig. 1, text class names are input into the text encoder to generate text embeddings $f^{t,e}$. The event data is encoded to produce the event embeddings f^e , and then the softmax function is applied to the final probability map generated by the multiplication between $f^{t,e}$ and f^e . In fine-tuning and few-shot event recognition scenarios, the former employs the entire training dataset, while the latter uses only a handful of training examples for each category during the training phase.

4.2 The Results for Event Recognition Task

Fine-tuning Setting. Fine-tuning experiment results are presented in Tab. 1 on N-Caltech101, N-MNIST, and N-ImageNet datasets compared with various baselines, including event self-supervised pre-training methods [32, 33, 38, 44, 53, 55, 66] and transfer learning of supervised image pretraining methods [21, 23, 40, 52, 62]. *our EventBind achieves new state-of-the-art accuracy compared with the previous method on three benchmarks by a large margin.* For N-Caltech101 dataset, our method achieves Top-1 accuracy of 95.29%, surpassing the previous SOTA [40] by +5.34% and competitor [64] by +1.72%. EventBind achieves 63.54% accuracy on N-ImageNet, an improvement of +4.79% over SOTA [32]. For N-MNIST, EventBind achieves SOTA accuracy of 99.45%, compared to 99.10% by [55]. The fine-tuning results prove EventBind’s superiority in effectively aligning event data with text and image. Our EventBind adapts well to datasets with various object classes, including 10, 101, and 1,000, demonstrating its transferability and robustness. We employ three versions with ViT backbones: ViT-B-32, ViT-B-16, and ViT-L-14. *See more discussion on model parameters with the different backbones in Sec.4.3.*

Few-shot Setting. We compare EventBind with existing methods, EventCLIP [64]. To ensure comparison consistency, the ViT-L-14 backbone is utilized

Table 1: Fine-tuned performance. ‘-’ represents the exact number not provided.

Method	Pretrain Dataset	Labels	Top-1 Accuracy (%)		
			N-Caltech101	N-MNIST	N-ImageNet
<i>Transfer learning of event self-supervised pre-training methods.</i>					
HATS [55]	✗	✗	64.20	99.10	47.14
AEGNN [53]	✗	✗	66.80	-	-
AsynNet [44]	✗	✗	74.50	-	-
EvS-S [38]	✗	✗	76.10	-	-
MEM [32]	NImNet-1k	✗	90.10	-	57.89
<i>Transfer learning of image supervised pre-training methods.</i>					
RG-CNN [7]	✗	✓	65.70	99.00	-
EST [21]	ImNet-1k	✓	81.70	-	48.93
DVS-ViT [62]	ImNet-21k	✓	83.00	-	-
Matrix-LSTM [9]	✗	✓	84.31	98.90	32.21
E2VID [52]	ImNet-1k	✓	86.60	98.30	-
DiST [29]	✗	✓	86.81	-	48.43
EventDrop [23]	ImNet-1k	✓	87.14	-	-
ACE-BET [40]	ImNet-1k	✓	89.95	-	-
<i>Transfer learning of image-text supervised pre-training methods.</i>					
EventCLIP(ViT-L-14) [64]	WIT	✓	93.57	-	53.20
EventBind(ours, ViT-B-32)	WIT	✓	93.74	99.26	42.94
EventBind(ours, ViT-B-16)	WIT	✓	94.08	99.27	51.40
EventBind(ours, ViT-L-14)	WIT	✓	95.29+1.72	99.45+0.35	63.54+5.65

Table 2: The few-shot Top-1 accuracy (%) compared with existing event-text model.

Setting	EventBind (Ours)			EventCLIP [64]	
	N-Caltech101	N-Imagenet	N-MNIST	N-Caltech101	N-Imagenet
5-shot	84.49+0.92	33.90+2.78	94.44	83.57	31.12
10-shot	88.73+1.31	36.97+2.73	95.76	87.42	34.24
20-shot	92.11+1.70	43.27+3.99	97.43	90.41	38.28

as EventCLIP stated. In Tab. 2, EventBind beats EventCLIP in few-shot cases, with gains of 0.92%, 1.31% and 1.7% for 5-shot, 10-shot, and 20-shot on N-Caltech101. Remarkably, our 20-shot accuracy outperforms the previous state-of-the-art (SOTA) [40], which was trained on the full dataset, while EventBind uses just 46.09% of the data from the N-Caltech101 dataset. For the N-ImageNet dataset, EventBind also outperforms EventCLIP with 2.78%, 2.73%, and 3.99% accuracy improvements for 5-shot, 10-shot, and 20-shot settings, showcasing its superiority in low-shot scenarios.

4.3 Ablation Study

Effectiveness of EventBind’s key components. Results in Tab. 3 demonstrate the HTCA module boosts performance by +42.14% and +77.72% on the N-Caltech and N-MNIST datasets. Text prompts further improve accuracy by +43.00% and +80.18%. Combining them with the proposed event encoder further increases accuracy to 93.87% and 99.20%, showing +43.68% and +80.50% gains, thus proving the effectiveness of EventBind’s key components.

Table 3: Ablation study on EventBind’s key components.

Ablation Settings			Top-1 Accuracy (%)	
HTCA	Text prompt	Event encoder	N-Caltech101	N-MNIST
\times	\times	\times	50.40	18.77
\checkmark	\times	\times	92.54+42.14	96.49+77.72
\checkmark	\checkmark	\times	93.40+43.00	98.95+80.18
\checkmark	\checkmark	\checkmark	94.08+43.68	99.27+80.50

Table 5: Ablation study on event encoder. P_e means event prompts.

Setting		Top-1 Accuracy (%)	
P_e	Event Temporal modeling	N-Caltech101	N-MNIST
\times	\times	90.40	95.78
\checkmark	\times	91.85+1.45	97.87+2.09
\times	\checkmark	92.27+1.87	98.22+2.44
\checkmark	\checkmark	94.08+3.68	99.27+3.49

The effectiveness of HTCA module In Tab. 4, loss $L(f^e, f^i)$ boosts accuracy by +19.91% and 39.18% on N-Caltech101 and N-MNIST. $L(f^e, f^{t,e})$ also enhances accuracy by +39.95% and 78.84%. EventBind combining $L(f^e, f^i)$ and $L(f^e, f^{t,e})$ achieves +42.71% and +80.25%, demonstrating the effectiveness of EventBind when the image inputs are not available with slightly performance loss compared with the full settings(-0.97%). With $L(f^{t,i}, f^{t,e})$, the whole HTCA module improves accuracy by +43.68% and +80.50%, showing the effectiveness of our proposed HTCA module.

The effectiveness of event encoder. In Tab. 5, event prompts P_e boost recognition accuracy by +1.45% and +2.09% on N-Caltech101 and N-MNIST datasets. Cross-frame prompts also enhance accuracy by +1.87% and +2.44%. Using both prompts together achieves +3.68% and +3.49% accuracy improvements. These results show the effectiveness of our event encoder.

Model parameter size analysis. We compare EventBind’s parameter size across different ViT backbones with the current event-text model [64] in Tab. 6. Given that EventCLIP can solely generate text and event embeddings, EventBind incorporates an additional image encoder to link events, images, and text. For a fair comparison, we present the parameter size of EventBind with and without the image encoder. In Tab. 6 and Tab. 1, EventBind (ViT-B-16) beats EventCLIP (ViT-L-14) on N-Caltech101 by 0.51% using only 71.3% of EventCLIP’s parameters (635MB V.S. 890MB), showing its superior efficiency.

The aggregated event counts per frame N . As shown in Fig. 4, we set N in training phrase based on the best zero-shot settings. We evaluate EventBind’s zero-shot capability against EventCLIP on identical N-Caltech101 validation datasets, maintaining the reported hyperparameters but substituting the event-to-frames codes. EventCLIP achieves 58.82% accuracy with 200,000 N , showing a -2.98% decrease in zero-shot accuracy, highlighting EventBind’s superiority.

Event representation. Tab. 7 displays the impact of different colorizing methods on frame-like event representations. Gray-scale achieves 92.18% and 97.61% accuracy, while RGB improves it to 94.08% and 99.27%.

Table 4: Ablation study on the HTCA module. ‘_’ highlights the EventBind performance in the absence of image inputs.

Ablation Settings			Top-1 Accuracy (%)	
$L(f^e, f^i)$	$L(f^e, f^{t,e})$	$L(f^{t,i}, f^{t,e})$	N-Caltech101	N-MNIST
\times	\times	\times	50.40	18.77
\checkmark	\times	\times	70.31+19.91	57.95+39.18
\times	\checkmark	\times	90.35+39.95	97.61+78.84
\checkmark	\checkmark	\times	93.11+42.71	99.02+80.25
\checkmark	\checkmark	\checkmark	94.08+43.68	99.27+80.50

Table 6: Model parameter analysis.

Backbone	ViT-L-14	ViT-B-32	ViT-B-16
EventCLIP [64]	890 MB	-	335 MB
EventBind (w.o Image Encoder)	1372 MB	474 MB	471 MB
EventBind (w.t. Image Encoder)	1952 MB	641 MB	635 MB

Table 7: Ablation study on training configuration & event frame representation.

Setting	Top-1 Accuracy (%)	
	N-Caltech101	N-MNIST
Frozen CLIP	86.69	97.11
Fine-tune CLIP	94.08	99.27
Gray-scale	92.18	97.61
RGB	94.08	99.27

Table 8: Ablation study on different hand-crafted text prompts.

Hand-crafted text prompts	Top-1 Accuracy (%)	
	N-Caltech101	N-MNIST
'A photo of a'	93.06	98.53
'A sketch image of a'	93.89	99.20
'A point cloud image of a'	92.71	98.49
'An event frame of a'	92.41	98.87
'A drafted image of a'	94.08	99.27

Table 9: Ablation study on the content prompts generation.

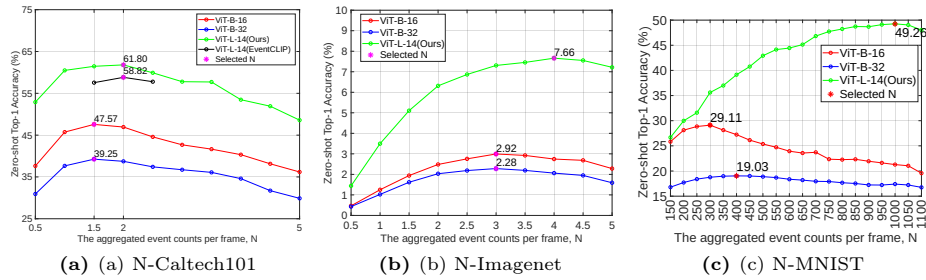
Ablation settings		Top-1 Accuracy (%)	
σ_i	σ_e	N-Caltech101	N-MNIST
\times	\times	91.96	98.51
\times	\checkmark	92.25+0.29	98.67+0.16
\checkmark	\times	92.82+0.86	98.72+0.21
\checkmark	\checkmark	94.08+2.12	99.27+0.76

Table 10: Ablation study on length of event modality prompts.

n_e	Top1 Accuracy	
	N-Caltech101	N-MNIST
4	93.27	97.95
8	93.89	98.73
16	94.08	99.27

Table 11: Ablation study on length of text learnable prompt.

n_l	Top1 Accuracy	
	N-Caltech101	N-MNIST
4	93.33	98.10
8	93.75	98.83
16	94.08	99.27

**Fig. 4:** Ablation of hyperparameters: the aggregated event counts per frame N based on zero-shot performance with 3 different ViT backbones across three datasets.

Fine-tune CLIP vs. Frozen CLIP as the event encoder backbone. In Tab. 7, we ablate to freeze and fine-tune the CLIP image encoder of Event Encoder. Using the frozen CLIP image encoder yields 86.69% and 97.11% accuracy while fine-tuning it raises accuracy to 94.08% and 99.27%, respectively.

The initialization of hand-crafted text prompts. We ablate five unique text prompts to determine which text embeddings best align with the event embeddings. The prompt 'A drafted image of a [class].' presents the best results of 94.08% and 99.27% on both N-Caltech101 and N-MNIST datasets.

The event and image content prompts. In Tab. 9, using the image content prompts σ_i alone boosts accuracy by +0.29% and +0.16% while employing the event content prompts σ_e alone improve accuracy by +0.86% and +0.21% on N-Caltech101 and N-MNIST datasets. Combining both yields a higher accuracy gain of +2.12% and +0.76%. Results show the effectiveness of our content prompt generation in boosting performance.

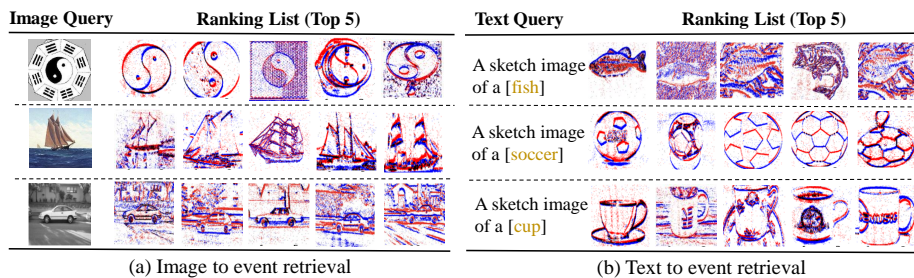


Fig. 5: Visual examples for the event retrieval task.

The length of text learnable prompts n_l . In Tab. 10, we evaluate different lengths of learnable text prompts, i.e., 4, 8, and 16. Using a length of 16 for the event modality prompts results in the highest recognition accuracy.

The length of event modality prompts n_e . In Tab. 11, We evaluate event modality prompts of varying lengths, namely 4, 8, and 16. Employing 16 as the prompt length yields the highest recognition accuracy.

4.4 Extension Experiment: Event Retrieval

EventBind can be expanded to image-to-event and text-to-event retrieval tasks. *See more details about event retrieval and results discussions in Suppl.* We initially perform the event retrieval task by employing both text and image queries. In Fig. 5, we present the Top-5 event data retrieved from the N-Caltech101 dataset using randomly selected images or class texts as queries. All the retrieved event data exhibit a very high degree of similarity to the input text query, showcasing the effectiveness of our proposed EventBind framework.

5 Conclusion and Future Work

In this paper, we tackled the challenge of generalizing CLIP to event modality, thus establishing a unified representation space among images, text, and events. To this end, we proposed EventBind, a novel framework that capitalizes on the potential of CLIP for event-based recognition tasks to compensate for the lack of large-scale event-based datasets. We introduced novel event encoders and text prompts designed to exploit the unique properties of event data and enhance its generalization ability. Furthermore, we proposed a hierarchical triple contrastive alignment to optimize the correlation alignment among these three distinct modalities. Extensive experiments on three object recognition benchmarks demonstrated the superiority and efficiency of EventBind. Extension experiments on event retrieval indicated it possesses excellent generalization ability.

Future work. We plan to extend EventBind to event-based downstream tasks. We hope that EventBind will facilitate the incorporation of knowledge from the text modality into the event-based vision, thereby harnessing decades of valuable research and contributing to the development of a more principled framework.

Acknowledgements

This paper is supported by the National Natural Science Foundation of China (NSF) under Grant No. NSFC22FYT45, the Guangzhou City, University and Enterprise Joint Fund under Grant No.SL2022A03J01278, and Guangzhou Fundamental and Applied Basic Research (Grant Number: 2024A04J4072)

Appendix

A. Preliminary of CLIP

The Contrastive Language-Image Pre-training (CLIP) [50] model is a prominent vision-language model that combines an image encoder (ViT [17] or ResNet [25]), with a text encoder based on the Transformer [57] architecture. CLIP focuses on generating visual and text embeddings and employs a contrastive loss to align these embeddings in a unified feature space. Notably, CLIP’s exceptional transferability is attributed to its pretraining on a large-scale dataset of more than four million image-text pairs.

For CLIP-based recognition, it usually employs a simple yet efficient method that takes N hand-crafted prompts like ‘a photo of a [cls]’ as the input for the text encoder to obtain the D -dimensional textual embedding $f^t \in \mathbb{R}^{N \times D}$, where [cls] is the class name and N is the number of classes of the downstream dataset. Meanwhile, for a given image, the visual embedding $f^i \in \mathbb{R}^{1 \times D}$ is obtained by the visual encoder. Then, the recognition logits $p \in \mathbb{R}^N$ can be obtained by calculating the similarity of text and visual embeddings by multiplication:

$$p = \text{Softmax}(f^i(f^t)^T), \quad (6)$$

where $\text{Softmax}(\cdot)$ denotes the Softmax function and p represents the predicted probability of the N classes. Finally, the highest scores of the logits p is regarded as the final prediction P :

$$P = \arg \max_{i \in \mathcal{N}} p_i \quad (7)$$

B. Implementation Details

Event Frame-like Representation Event cameras capture object movement by detecting temporal independence and recording pixel-level brightness changes. The event stream, denoted as $\mathcal{E} = e_i(x_i, y_i, t_i, p_i)$, reflects the brightness change e_i of a pixel at the timestamp t_i , with coordinates (x_i, y_i) , and polarity $p_i \in \{1, -1\}$. Here, 1 and -1 represent the positive and negative intensity change of brightness, respectively. We convert the event stream into a sequence of frames. First, we normalize the length of the event stream \mathcal{E} to a fixed amount P using zero-padding or taking the first P events. Then, we group every Q consecutive event

Backbone	N-Imagnet	N-MNIST	N-Caltech101
ViT-B-16	300,000	300	150,000
ViT-B-32	300,000	400	150,000
ViT-L-14	400,000	1,000	200,000

Table 12: The settings of aggregated event counts per frame N for different backbones on three datasets.

data in the normalized event stream \mathcal{E}' to obtain event parts $\mathcal{E}'' \in \mathbb{R}^{T \times 4 \times P}$, where $T = P/Q$ and denotes the number of event frames.

We then transform these event parts into histograms $h \in \mathbb{R}^{T \times H \times W \times 2}$ by counting the amount of positive and negative events per pixel, where H and W represent the height and width of an event frame, respectively. Finally, to attain the grid-like 3-channel input $I_e \in \mathbb{R}^{T \times H \times W \times 3}$, we colorize the t th event histogram h_t by multiplying the predefined red color map $[0, 255, 255]$ and blue color map $[255, 255, 0]$ with the positive and negative event histogram respectively and merge them by pixel-wise addition, which can be formulated as follow:

$$I_{e,t} = h_t^p[0, 255, 255]^T + h_t^n[255, 255, 0]^T, \quad (8)$$

where the $I_{e,t}$ represents the event input for the t th event frame and $t = 0, 1, \dots, T$; h_t^p and h_t^n denotes the positive and negative event histogram respectively. Finally, the generated event frame input is resized into the 224×224 resolution for adapting to the ViT setting, generating the final event input $I'_e \in \mathbb{R}^{T \times 224 \times 224 \times 3}$.

The above grid-like event representation is simple yet effective since the generated event image resembles the edge image, whose data distribution is much closer to the pre-trained natural images so that the transfer pressure is erased and the modality gap is bridged.

Additional Dataset Settings **N-ImageNet** [29] is derived from ImageNet-1K dataset, where the RGB images are displayed on a monitor and captured by a moving event camera. It includes 1,781,167 event streams with 480×640 resolution across 1,000 unique object classes. **N-Caltech101** [19] contains event streams captured by an event camera in front of a mobile 180×240 ATIS system [49] with the LCD monitor presenting the original RGB images in Caltech101. There are 8,246 samples comprising 300 ms in length, covering 101 different types of items. **N-MNIST** is created by displaying a moving image from the MNIST dataset on the ATIS system with the LCD monitor. It contains 70,000 event data samples covering 10 handwritten numbers from 0 to 9.

Additional Experimental Settings We use "A drafted image of a [CLS]" as the hand-crafted text prompts template. The Pytorch [48] framework serves as the foundation for all experiments. The initial learning rates are set to $1e-5$ for the N-Caltech101 dataset and $1e-6$ for the N-Imagnet and N-MNIST datasets. The weight decay is $2e-4$. CosineAnnealingLR [42] learning rate schedule is utilized, and the minimal learning rate is $1e-8$. All few-shot and fine-tuning experiments

Ablation settings		Base		New	
Learnable	Hand-crafted	N-Caltech101	N-MNIST	N-Caltech101	N-MNIST
✗	✓	90.57	91.03	72.55	18.80
✓	✗	91.01	93.22	61.85	46.02
✓	✓	91.23	93.56	68.02	49.92

Table 13: Ablation study on hybrid text prompts module.

are trained for 30 epochs with Adam [30] optimizer. Unless specified otherwise, the ablation study is conducted on the N-Caltech101/Caltech101 datasets utilizing ViT-B-16 [16] image encoder and the Transformer-based text encoder [57] as the backbone. The event encoder is initialized with the CLIP image encoder’s pre-trained weights and is fine-tuned during training. We choose the aggregated event counts per frame N based on the best EventBind’s zero-shot performance. Tab. 12 represents the value of N set for different backbones on three datasets.

C. Additional Experiment Result

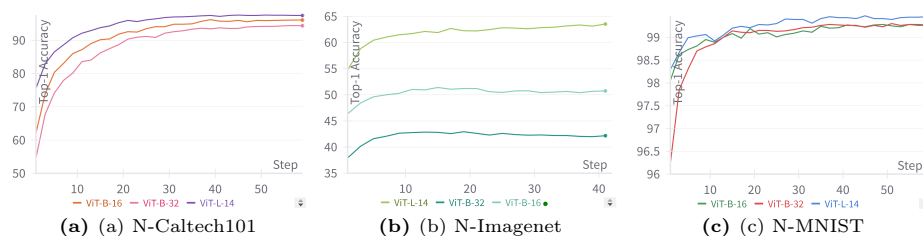
The Effectiveness of Hybrid Text Prompts We ablated the hybrid text prompts to evaluate their impact on fine-tuning performance and generalization ability. The experiment follows the setting proposed in [75], where the entire dataset is divided into the base and new datasets, each containing half of the object classes. For each ablation setting, the model is fine-tuned on the base set without being exposed to half of the event classes in the new set. The evaluation is then performed on the new set to assess the generalization ability.

As shown in Tab. 13, the hand-crafted text prompts achieve an impressive 72.55% Top-1 accuracy on the new set for the N-Caltech101 dataset, showcasing its remarkable zero-shot ability. In contrast, while learnable text prompts boost fine-tuning performance on the base set, they lead to decreased accuracy on the new set due to limited generalization capabilities. *In contrast, our proposed hybrid text prompts module, which integrates both learnable and manually-crafted text prompts, attains the highest fine-tuning accuracy of 91.23% while exhibiting a smaller decrease in zero-shot performance relative to solely utilizing single hand-crafted text prompts. (-10.70% V.S -4.53% for N-Caltech101).* For the N-MNIST dataset, it’s expected that the model exhibits low accuracy on the base dataset with hand-crafted text prompts. This stems from the subpar image recognition capability of the original CLIP on N-MNIST, where zero-shot CLIP results are 10% inferior to those of the linear probe on ResNet50 for MNIST. [50]). *Our model, equipped with the hybrid text prompts module, secures top-one accuracy on both the base dataset (93.56%) and the new dataset (98.86%) for N-MNIST, underscoring the effectiveness of our proposed module.* **Zero-shot, 1-shot, 2-shot Results Compared with EventCLIP.** Since the dataset split of EventCLIP for 1-shot and 2-shot is unavailable, we evaluated it on our dataset split with ViT-L-14 backbones. As shown in Tab. 14, our EventBind achieves better zero-shot, 1-shot, and 2-shot performance than EventCLIP.

Setting	EventBind (scratch)		EventCLIP (scratch)	
	N-Caltech101	N-MINIST	N-Caltech101	N-MINIST
0-shot	61.80	56.81	58.82	48.72
1-shot	74.96	74.64	70.53	74.62
2-shot	79.78	82.89	77.71	82.78

Table 14: The zero-shot and few-shot results.

Model	E2VID [52]	SSL-E2VID [47]	Wang et al. [59]	Ev-LaFOR [12]	EventBind(Ours)
Top1 Accuracy	61.7	25.3	48.5	85.56	86.02

Table 15: Open-vocabulary results on N-Caltech101.**Fig. 6:** The Accuracy curves with three ViT backbones on the N-MINIST, N-Caltech101, and N-Imagenet datasets.

Setting	Text2Event			Imgae2Event		
	Recall@1	Recall@5	Recall@10	Recall@1	Recall@5	Recall@10
0-shot	78.22	88.12	91.09	79.40	90.34	93.58
1-shot	81.19	95.05	98.02	82.75	96.04	99.01
2-shot	90.10	99.01	100.00	88.31	98.02	99.01
5-shot	97.03	100.00	100.00	90.97	99.01	100.00
10-shot	98.02	100.00	100.00	94.73	99.01	100.00
20-shot	99.01	100.00	100.00	96.70	100.00	100.00
Fine-tune	100.00	100.00	100.00	96.88	99.60	99.95

Table 16: Event Retrieval Results on N-Caltech101 Dataset with Zero-shot, Few-shot, and Fine-tuning Settings.

Open-vocabulary Recognition Result For open-vocabulary event recognition, the text classes are arbitrary rather than restricted to the training classes. We follow the dataset split based on its open-source repository. The results are in Tab. 15. Our EventBind achieves the SoTA performance of **86.02%**, proving its superiority for open-vocabulary recognition.

Accuracy Curve We present the training accuracy curves trained by employing three ViT backbones on the N-MINIST, N-Caltech101, and N-Imagenet datasets in Fig. 6. As the number of training epochs increases, the accuracy of the model increases steadily, demonstrating the stability and reproducibility of EventBind.

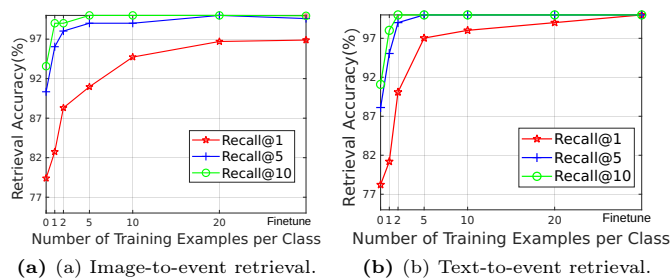


Fig. 7: Event retrieval results on N-Caltech101 dataset with zero-shot, few-shot, and fine-tuning settings.

Event Retrieval Numerical Results We utilize Recall@1, Recall@5, and Recall@10 metrics commonly employed in retrieval tasks [11, 69]. In Fig. 7, our EventBind shows remarkable retrieval performance (99.01% Recall@1 for text query and 96.70% Recall@1 for image query) with only 20 shot training examples, demonstrating its remarkable capabilities in few-shot learning. Notably, our model excels in text-to-event and image-to-event retrieval, achieving recall rates close to 100.00% on Recall@1 after fine-tuning. This exceptional performance demonstrates that EventBind effectively establishes a unified representation space with aligned event, images and text embeddings. To ease future comparison, we report all those numbers in Tab. 16.

References

1. Amir, A., Taba, B., Berg, D., Melano, T., McKinstry, J., Di Nolfo, C., Nayak, T., Andreopoulos, A., Garreau, G., Mendoza, M., et al.: A low power, fully event-based gesture recognition system. In: CVPR (2017)
2. Ba, J.L., Kiros, J.R., Hinton, G.E.: Layer normalization. arXiv preprint arXiv:1607.06450 (2016)
3. Bahng, H., Jahanian, A., Sankaranarayanan, S., Isola, P.: Exploring visual prompts for adapting large-scale models. arXiv preprint arXiv:2203.17274 (2022)
4. Bai, Y., Wang, C., Xie, S., Dong, C., Yuan, C., Wang, Z.: Textir: A simple framework for text-based editable image restoration. arXiv preprint arXiv:2302.14736 (2023)
5. Baldwin, R.W., Almatrafi, M., Kaufman, J.R., Asari, V., Hirakawa, K.: Inceptive event time-surfaces for object classification using neuromorphic cameras. In: ICIAR (2019)
6. Bar, A., Gandelsman, Y., Darrell, T., Globerson, A., Efros, A.: Visual prompting via image inpainting. *Advances in Neural Information Processing Systems* **35**, 25005–25017 (2022)
7. Bi, Y., Chadha, A., Abbas, A., Bourtsoulatze, E., Andreopoulos, Y.: Graph-based object classification for neuromorphic vision sensing. In: Proceedings of the IEEE/CVF international conference on computer vision. pp. 491–501 (2019)
8. Botzheim, J., Obo, T., Kubota, N.: Human gesture recognition for robot partners by spiking neural network and classification learning. In: SCIS (2012)

9. Cannici, M., Ciccone, M., Romanoni, A., Matteucci, M.: A differentiable recurrent surface for asynchronous event-based data. In: *Computer Vision–ECCV 2020: 16th European Conference, Glasgow, UK, August 23–28, 2020, Proceedings, Part XX 16*. pp. 136–152. Springer (2020)
10. Chen, F.L., Zhang, D.Z., Han, M.L., Chen, X.Y., Shi, J., Xu, S., Xu, B.: Vlp: A survey on vision-language pre-training. *Machine Intelligence Research* **20**(1), 38–56 (2023)
11. Chen, X., Fang, H., Lin, T.Y., Vedantam, R., Gupta, S., Dollár, P., Zitnick, C.L.: Microsoft coco captions: Data collection and evaluation server. *arXiv preprint arXiv:1504.00325* (2015)
12. Cho, H., Kim, H., Chae, Y., Yoon, K.J.: Label-free event-based object recognition via joint learning with image reconstruction from events. In: *Proceedings of the IEEE/CVF International Conference on Computer Vision*. pp. 19866–19877 (2023)
13. Deng, J., Dong, W., Socher, R., Li, L.J., Li, K., Fei-Fei, L.: Imagenet: A large-scale hierarchical image database. In: *2009 IEEE conference on computer vision and pattern recognition*. pp. 248–255. Ieee (2009)
14. Deng, L.: The mnist database of handwritten digit images for machine learning research [best of the web]. *IEEE signal processing magazine* **29**(6), 141–142 (2012)
15. Deng, Y., Chen, H., Liu, H., Li, Y.: A Voxel Graph CNN for Object Classification With Event Cameras. In: *CVPR* (2022)
16. Dosovitskiy, A., Beyer, L., Kolesnikov, A., Weissenborn, D., Zhai, X., Unterthiner, T., Dehghani, M., Minderer, M., Heigold, G., Gelly, S., et al.: An image is worth 16x16 words: Transformers for image recognition at scale. *arxiv 2020*. *arXiv preprint arXiv:2010.11929* (2010)
17. Dosovitskiy, A., Beyer, L., Kolesnikov, A., Weissenborn, D., Zhai, X., Unterthiner, T., Dehghani, M., Minderer, M., Heigold, G., Gelly, S., et al.: An image is worth 16x16 words: Transformers for image recognition at scale. *arXiv preprint arXiv:2010.11929* (2020)
18. Du, Y., Liu, Z., Li, J., Zhao, W.X.: A survey of vision-language pre-trained models. *arXiv preprint arXiv:2202.10936* (2022)
19. Fei-Fei, L., Fergus, R., Perona, P.: Learning generative visual models from few training examples: An incremental bayesian approach tested on 101 object categories. In: *2004 conference on computer vision and pattern recognition workshop*. pp. 178–178. IEEE (2004)
20. Gallego, G., Delbrück, T., Orchard, G., Bartolozzi, C., Taba, B., Censi, A., Leutenegger, S., Davison, A.J., Conradt, J., Daniilidis, K., et al.: Event-based vision: A survey. *IEEE transactions on pattern analysis and machine intelligence* **44**(1), 154–180 (2020)
21. Gehrig, D., Loquercio, A., Derpanis, K.G., Scaramuzza, D.: End-to-end learning of representations for asynchronous event-based data. In: *Proceedings of the IEEE/CVF International Conference on Computer Vision*. pp. 5633–5643 (2019)
22. Gehrig, D., Loquercio, A., Derpanis, K.G., Scaramuzza, D.: End-to-end learning of representations for asynchronous event-based data. In: *ICCV* (2019)
23. Gu, F., Sng, W., Hu, X., Yu, F.: Eventdrop: Data augmentation for event-based learning. *arXiv preprint arXiv:2106.05836* (2021)
24. Gu, F., Sng, W., Taunyazov, T., Soh, H.: Tactilesgnet: A spiking graph neural network for event-based tactile object recognition. In: *IROS* (2020)
25. He, K., Zhang, X., Ren, S., Sun, J.: Deep residual learning for image recognition. In: *Proceedings of the IEEE conference on computer vision and pattern recognition*. pp. 770–778 (2016)

26. Herzig, R., Abramovich, O., Ben-Avraham, E., Arbelle, A., Karlinsky, L., Shamir, A., Darrell, T., Globerson, A.: Promptonomyvit: Multi-task prompt learning improves video transformers using synthetic scene data. arXiv preprint arXiv:2212.04821 (2022)
27. Huang, X., Li, S., Qu, W., He, T., Zuo, Y., Ouyang, W.: Frozen clip model is efficient point cloud backbone. arXiv preprint arXiv:2212.04098 (2022)
28. Jia, M., Tang, L., Chen, B.C., Cardie, C., Belongie, S., Hariharan, B., Lim, S.N.: Visual prompt tuning. In: European Conference on Computer Vision. pp. 709–727. Springer (2022)
29. Kim, J., Bae, J., Park, G., Zhang, D., Kim, Y.M.: N-imagenet: Towards robust, fine-grained object recognition with event cameras. In: Proceedings of the IEEE/CVF international conference on computer vision. pp. 2146–2156 (2021)
30. Kingma, D.P., Ba, J.: Adam: A method for stochastic optimization. arXiv preprint arXiv:1412.6980 (2014)
31. Kirillov, A., Mintun, E., Ravi, N., Mao, H., Rolland, C., Gustafson, L., Xiao, T., Whitehead, S., Berg, A.C., Lo, W.Y., et al.: Segment anything. arXiv preprint arXiv:2304.02643 (2023)
32. Klenk, S., Bonello, D., Koestler, L., Araslanov, N., Cremers, D.: Masked event modeling: Self-supervised pretraining for event cameras. In: Proceedings of the IEEE/CVF Winter Conference on Applications of Computer Vision. pp. 2378–2388 (2024)
33. Klenk, S., Bonello, D., Koestler, L., Cremers, D.: Masked event modeling: Self-supervised pretraining for event cameras. arXiv preprint arXiv:2212.10368 (2022)
34. Lagorce, X., Orchard, Garrick and Galluppi, F., Shi, B.E., Benosman, R.B.: Hots: a hierarchy of event-based time-surfaces for pattern recognition. TPAMI (2016)
35. Li, D., Li, J., Li, H., Niebles, J.C., Hoi, S.C.: Align and prompt: Video-and-language pre-training with entity prompts. In: Proceedings of the IEEE/CVF Conference on Computer Vision and Pattern Recognition. pp. 4953–4963 (2022)
36. Li, J., Li, D., Savarese, S., Hoi, S.: Blip-2: Bootstrapping language-image pre-training with frozen image encoders and large language models. arXiv preprint arXiv:2301.12597 (2023)
37. Li, X., Yin, X., Li, C., Zhang, P., Hu, X., Zhang, L., Wang, L., Hu, H., Dong, L., Wei, F., et al.: Oscar: Object-semantics aligned pre-training for vision-language tasks. In: Computer Vision–ECCV 2020: 16th European Conference, Glasgow, UK, August 23–28, 2020, Proceedings, Part XXX 16. pp. 121–137. Springer (2020)
38. Li, Y., Zhou, H., Yang, B., Zhang, Y., Cui, Z., Bao, H., Zhang, G.: Graph-based asynchronous event processing for rapid object recognition. In: Proceedings of the IEEE/CVF International Conference on Computer Vision. pp. 934–943 (2021)
39. Lin, Z., Geng, S., Zhang, R., Gao, P., de Melo, G., Wang, X., Dai, J., Qiao, Y., Li, H.: Frozen clip models are efficient video learners. In: European Conference on Computer Vision. pp. 388–404. Springer (2022)
40. Liu, C., Qi, X., Lam, E.Y., Wong, N.: Fast classification and action recognition with event-based imaging. IEEE Access **10**, 55638–55649 (2022)
41. Liu, M., Zhu, Y., Cai, H., Han, S., Ling, Z., Porikli, F., Su, H.: Partslip: Low-shot part segmentation for 3d point clouds via pretrained image-language models. In: Proceedings of the IEEE/CVF Conference on Computer Vision and Pattern Recognition. pp. 21736–21746 (2023)
42. Loshchilov, I., Hutter, F.: Sgdr: Stochastic gradient descent with warm restarts. arXiv preprint arXiv:1608.03983 (2016)

43. Mahmud, T., Marculescu, D.: Ave-clip: Audioclip-based multi-window temporal transformer for audio visual event localization. In: Proceedings of the IEEE/CVF Winter Conference on Applications of Computer Vision. pp. 5158–5167 (2023)
44. Messikommer, N., Gehrig, D., Loquercio, A., Scaramuzza, D.: Event-based asynchronous sparse convolutional networks. In: Computer Vision–ECCV 2020: 16th European Conference, Glasgow, UK, August 23–28, 2020, Proceedings, Part VIII 16. pp. 415–431. Springer (2020)
45. Ni, B., Peng, H., Chen, M., Zhang, S., Meng, G., Fu, J., Xiang, S., Ling, H.: Expanding language-image pretrained models for general video recognition. In: Computer Vision–ECCV 2022: 17th European Conference, Tel Aviv, Israel, October 23–27, 2022, Proceedings, Part IV. pp. 1–18. Springer (2022)
46. Orchard, G., Jayawant, A., Cohen, G.K., Thakor, N.: Converting static image datasets to spiking neuromorphic datasets using saccades. *Frontiers in neuroscience* **9**, 437 (2015)
47. Paredes-Vallés, F., De Croon, G.C.: Back to event basics: Self-supervised learning of image reconstruction for event cameras via photometric constancy. In: Proceedings of the IEEE/CVF Conference on Computer Vision and Pattern Recognition. pp. 3446–3455 (2021)
48. Paszke, A., Gross, S., Massa, F., Lerer, A., Bradbury, J., Chanan, G., Killeen, T., Lin, Z., Gimelshein, N., Antiga, L., et al.: Pytorch: An imperative style, high-performance deep learning library. *Advances in neural information processing systems* **32** (2019)
49. Posch, C., Matolin, D., Wohlgenannt, R.: A qvga 143 db dynamic range frame-free pwm image sensor with lossless pixel-level video compression and time-domain cds. *IEEE Journal of Solid-State Circuits* **46**(1), 259–275 (2010)
50. Radford, A., Kim, J.W., Hallacy, C., Ramesh, A., Goh, G., Agarwal, S., Sastry, G., Askell, A., Mishkin, P., Clark, J., et al.: Learning transferable visual models from natural language supervision. In: International conference on machine learning. pp. 8748–8763. PMLR (2021)
51. Rasheed, H., Khattak, M.U., Maaz, M., Khan, S., Khan, F.S.: Fine-tuned clip models are efficient video learners. In: Proceedings of the IEEE/CVF Conference on Computer Vision and Pattern Recognition. pp. 6545–6554 (2023)
52. Rebecq, H., Ranftl, R., Koltun, V., Scaramuzza, D.: Events-to-video: Bringing modern computer vision to event cameras. In: Proceedings of the IEEE/CVF Conference on Computer Vision and Pattern Recognition. pp. 3857–3866 (2019)
53. Schaefer, S., Gehrig, D., Scaramuzza, D.: Aegnn: Asynchronous event-based graph neural networks. In: Proceedings of the IEEE/CVF conference on computer vision and pattern recognition. pp. 12371–12381 (2022)
54. Shen, S., Yang, S., Zhang, T., Zhai, B., Gonzalez, J.E., Keutzer, K., Darrell, T.: Multitask vision-language prompt tuning. *arXiv preprint arXiv:2211.11720* (2022)
55. Sironi, A., Brambilla, M., Bourdis, N., Lagorce, X., Benosman, R.: HATS: Histograms of averaged time surfaces for robust event-based object classification. In: CVPR (2018)
56. Tsimpoukelli, M., Menick, J.L., Cabi, S., Eslami, S., Vinyals, O., Hill, F.: Multimodal few-shot learning with frozen language models. *Advances in Neural Information Processing Systems* **34**, 200–212 (2021)
57. Vaswani, A., Shazeer, N., Parmar, N., Uszkoreit, J., Jones, L., Gomez, A.N., Kaiser, Ł., Polosukhin, I.: Attention is all you need. *Advances in neural information processing systems* **30** (2017)

58. Wang, J., Zhou, P., Shou, M.Z., Yan, S.: Position-guided text prompt for vision-language pre-training. In: Proceedings of the IEEE/CVF Conference on Computer Vision and Pattern Recognition. pp. 23242–23251 (2023)
59. Wang, L., Ho, Y.S., Yoon, K.J., et al.: Event-based high dynamic range image and very high frame rate video generation using conditional generative adversarial networks. In: Proceedings of the IEEE/CVF Conference on Computer Vision and Pattern Recognition. pp. 10081–10090 (2019)
60. Wang, Y., Du, B., Shen, Y., Wu, K., Zhao, G., Sun, J., Wen, H.: EV-Gait: Event-based robust gait recognition using dynamic vision sensors. In: CVPR (2019)
61. Wang, Z., Yu, J., Yu, A.W., Dai, Z., Tsvetkov, Y., Cao, Y.: Simvlm: Simple visual language model pretraining with weak supervision. arXiv preprint arXiv:2108.10904 (2021)
62. Wang, Z., Hu, Y., Liu, S.C.: Exploiting spatial sparsity for event cameras with visual transformers. In: 2022 IEEE International Conference on Image Processing (ICIP). pp. 411–415. IEEE (2022)
63. Wasim, S.T., Naseer, M., Khan, S., Khan, F.S., Shah, M.: Vita-clip: Video and text adaptive clip via multimodal prompting. In: Proceedings of the IEEE/CVF Conference on Computer Vision and Pattern Recognition. pp. 23034–23044 (2023)
64. Wu, Z., Liu, X., Gilitschenski, I.: Eventclip: Adapting clip for event-based object recognition. arXiv preprint arXiv:2306.06354 (2023)
65. Xue, L., Gao, M., Xing, C., Martín-Martín, R., Wu, J., Xiong, C., Xu, R., Niebles, J.C., Savarese, S.: Ulip: Learning a unified representation of language, images, and point clouds for 3d understanding. In: Proceedings of the IEEE/CVF Conference on Computer Vision and Pattern Recognition. pp. 1179–1189 (2023)
66. Yang, Y., Pan, L., Liu, L.: Event camera data pre-training. arXiv preprint arXiv:2301.01928 (2023)
67. Yao, H., Zhang, R., Xu, C.: Visual-language prompt tuning with knowledge-guided context optimization. In: Proceedings of the IEEE/CVF Conference on Computer Vision and Pattern Recognition. pp. 6757–6767 (2023)
68. Yao, Y., Zhang, A., Zhang, Z., Liu, Z., Chua, T.S., Sun, M.: Cpt: Colorful prompt tuning for pre-trained vision-language models. arXiv preprint arXiv:2109.11797 (2021)
69. Young, P., Lai, A., Hodosh, M., Hockenmaier, J.: From image descriptions to visual denotations: New similarity metrics for semantic inference over event descriptions. *Transactions of the Association for Computational Linguistics* **2**, 67–78 (2014)
70. Zang, Y., Li, W., Zhou, K., Huang, C., Loy, C.C.: Unified vision and language prompt learning. arXiv preprint arXiv:2210.07225 (2022)
71. Zeng, Y., Jiang, C., Mao, J., Han, J., Ye, C., Huang, Q., Yeung, D.Y., Yang, Z., Liang, X., Xu, H.: Clip2: Contrastive language-image-point pretraining from real-world point cloud data. In: Proceedings of the IEEE/CVF Conference on Computer Vision and Pattern Recognition. pp. 15244–15253 (2023)
72. Zhang, R., Guo, Z., Zhang, W., Li, K., Miao, X., Cui, B., Qiao, Y., Gao, P., Li, H.: Pointclip: Point cloud understanding by clip. In: Proceedings of the IEEE/CVF Conference on Computer Vision and Pattern Recognition. pp. 8552–8562 (2022)
73. Zhang, R., Zeng, Z., Guo, Z., Li, Y.: Can language understand depth? In: Proceedings of the 30th ACM International Conference on Multimedia. pp. 6868–6874 (2022)
74. Zheng, X., Liu, Y., Lu, Y., Hua, T., Pan, T., Zhang, W., Tao, D., Wang, L.: Deep learning for event-based vision: A comprehensive survey and benchmarks. arXiv preprint arXiv:2302.08890 (2023)

75. Zhou, K., Yang, J., Loy, C.C., Liu, Z.: Conditional prompt learning for vision-language models. In: Proceedings of the IEEE/CVF Conference on Computer Vision and Pattern Recognition. pp. 16816–16825 (2022)
76. Zhou, K., Yang, J., Loy, C.C., Liu, Z.: Learning to prompt for vision-language models. *International Journal of Computer Vision* **130**(9), 2337–2348 (2022)